Micromechanisms of High-Energy Peel Failure in Polyester–Aluminum–Polyester Laminates

D. J. BROWN,* P. LAMB, and A. H. WINDLE, *Department of Materials Science and Metallurgy, University of Cambridge, Cambridge CB2 3QZ, United Kingdom*

Synopsis

Symmetrical polyester-aluminum-polyester laminates are prepared using poly(ethylene terephthalate) film subjected to a glow discharge pretreatment. Extremely high peel energies (several hundred J m^{-2}) are achieved, and the fracture path is principally cohesive: the laminate performance thus fully exploits the bulk mechanical properties of the PET. The peel surface exhibits extensive plasticity on a scale of tens of microns, with finer ductile tearing on a scale of order 1 μm. The mechanism of peel propagation and energy dissipation is discussed with regard to the optimisation of peel strength.

INTRODUCTION

Previous publications from the authors' laboratory[1-3] have described the fabrication and testing of symmetrical polyester–aluminum–polyester laminates, produced by the thermal evaporation of aluminum on to the surfaces of strips of poly(ethylene terephthalate) (PET) film immediately before they are brought together under vacuum in a roll nip. The method is illustrated in Figure 1. This polymer–metal–polymer (PMP) geometry has the advantage that the metal layer is fully protected from abrasion, a potentially important feature in performance packaging applications; it also provides a valuable method of sample preparation for the study of metal–polyester, adhesion, and peel behavior. The latter aspect is the subject of the present paper.

A strict definition of the term "adhesion" reserves its use to bonding at a clearly defined interface between two materials; the term "adhesive energy" used in a thermodynamic sense implies that bonding is a reversible process and that there is intimate contact at the interface. These idealized conditions are not realized in metallized polyester film. Also, there are considerable practical difficulties in measuring these quantities, for instance in defining the area of perfect contact, or in applying a force to separate the two materials without introducing additional mechanisms of energy storage or dissipation. Many methods which purport to give measures of "adhesion" in fact introduce energy-dissipative mechanisms which are quite additional to those genuinely associated with the adhesive bond. For example, perhaps the most

* Now at: ICI PLC, Biological Products Business, PO Box 1, Billingham, Cleveland TS23 1LB, U.K.

Journal of Applied Polymer Science, Vol. 35, 279–297 (1988)
 CCC 0021-8995/88/020279-19$04.00

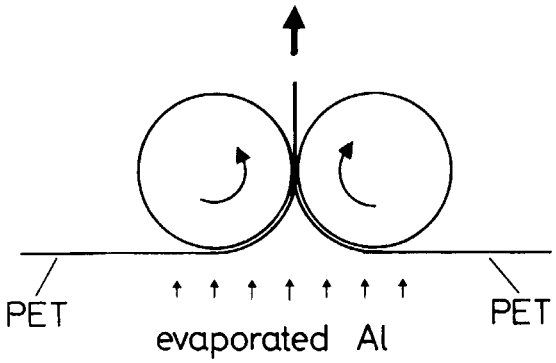

Fig. 1. The production of a polymer–metal–polymer laminate.

common test for a metallized polymer film is to stick a strip of proprietary adhesive tape on to the metal coating and measure the force required to pull it off: Provided that most or all of the metal is removed along with the tape, this force is then used as a measure of adhesive strength. Such a test breaks down in the common situation where peel failure takes place at the metal/adhesive interface or cohesively within the adhesive layer; the metal coating is not removed and an upper limit is imposed on the value which can be measured. Furthermore, in, for example, a test on metallized PET, much the greater part of the measured force is accounted for by deformation of the tape adhesive.

In the PMP geometry the need to add additional adhesive material is avoided and extraneous contribution to the measured peel energy are thus eliminated. The possibility that bulk dissipative losses occur within the films as a consequence of the bending and stretching associated with the T peel geometry remains. However, for the film thicknesses used, 50 μm biaxially drawn polyester, the in-plane tensile stresses were very much lower than the tensile yield stress of the film (0–10%), and bulk contributions to the measured energies will be small. There was also no consequence of the test.

As the fabrication of the PMP laminate involves metallization, it cannot provide a "quality control" test for premetallized material. Its particular value is that it entitles one to relate measured peel energies to the underlying mechanisms of deformation in a symmetrical sample (Fig. 2). The ability to examine the peel behavior of strongly bonded peel systems—well beyond the range of the "tape" test—has proved especially useful, and this paper describes studies on laminates with peel energies of several hundred J m^{-2}.

EXPERIMENTAL

Materials

The PET film used was cut from a reel of 50 μm thick ICI "Melinex" Type O, an unfilled additive-free grade produced by biaxial drawing. Examination by reflection Nomarski differential interference microscopy revealed no evidence of surface relief, though transmission microscopy between crossed polars revealed a distribution of point features presumably associated with dust particles[4] included during processing or subsequent reeling (Fig. 3).

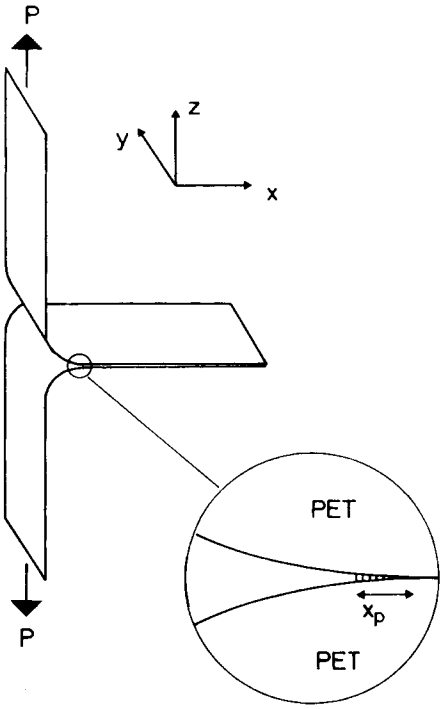

Fig. 2. Geometry of the T-peel test. The short-range nature of intermolecular forces across the failure path mean that to a good approximation the peel force P is supported over an area extending across the width of the specimen in the y-direction, but with a dimension x_p in the x-direction, which is only comparable to molecular spacings.

The aluminum used was supplied by Johnson Matthew Chemicals Ltd. in rod form, 6 mm diameter. The impurities detected were limited to silicon (10 ppm), copper and iron (1 ppm), calcium, magnesium, and silver (< 1 ppm).

Lamination Procedure

PET–aluminum–PET laminates were prepared in a modified Edwards 306 coater according to the method described previously.[1,2] The glow discharge pretreatment was carried out for 2 min at an initial pressure of 6×10^{-3} mbar of air; the distance between the sample and the glow discharge electrode was 15–20 cm. X-ray photoelectron spectroscopy indicates that such a pretreatment has the dual effect of surface cleaning and of the introduction of additional oxygen functionalities, notably hydroxyl groups, at the PET surface.[2,5] Metallization was carried out at an initial pressure of 10^{-5} mbar of air with a deposition rate of 25 nm s^{-1}, giving a total metal thickness of several tens of nanometers. The film was shielded from radiant heat until immediately before deposition. The two films were laminated at a roll pressure of 5×10^5 N/m^2 and the film speed was 4 cm/s.

Peel Testing

Strips of width 1 cm were cut from the laminate parallel to the feed-through direction, and subjected to a T-peel test at room temperature with crosshead

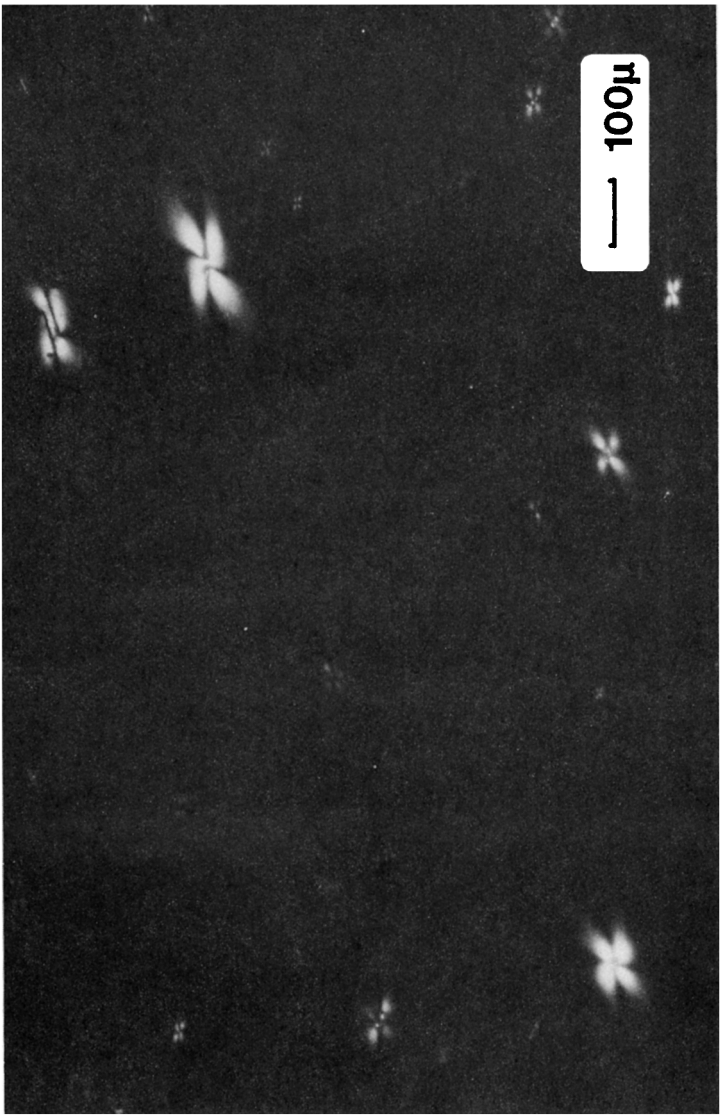

Fig. 3. Transmission optical micrograph of 50u Melinex PET film between crossed polars. The PET film is in an extinction position for regions remote from dust particles.

speed 5 mm s^{-1} (so that the peel failure propagates at 2.5 mm s^{-1}). Peel tests were performed either in a bench-top peel tester (Instrumentors, Inc., Cleveland, OH, slip-peel tester Model SP-101 A), or in an Instron model 1026 displacement-controlled mechanical testing machine. Peak and mean peel forces were recorded; it is helpful to note that the peel force (g/cm width of strip) is numerically nearly the same as the energy per unit area of failure surface created (i.e. half the energy per unit original laminate area) (J/m^2). Sections of the failure surfaces were mounted for SEM examination and lightly sputter-coated with gold to avoid charging in the electron beam. Viewed edge-on, an advancing peel front looks like a propagating crack, and we will refer to it accordingly.

The Laminate Failure Energy

As in many adhesive bonding situations it is essential to distinguish between the intrinsic adhesive bond energy and the fracture energy. The former may be defined as the energy lost on bringing two surfaces together from infinity to form an interface: If failure were a simple reversal of this process, the work required would be fully accounted for by the creation of two free surfaces, and the recorded peel energy could be equated to the net change in surface energy. Similarly, for a reversible cohesive failure process, the peel energy would be equal to twice the surface energy of the solid. At any instant during a peel test the applied force is effectively concentrated on a very small area of the bond by the geometry of the crack (Fig. 2), which for the reversible case would be atomically sharp. Thus the peel force should, for these mechanisms, be extremely small. PET has a surface energy of 47 mJ m^{-2},[6] which would suggest peel energies below about 0.1 J m^{-2}, i.e., peel forces less than 0.1 N m width of film!

Practical systems display failure energies vastly higher than this (over 600 J m^{-2} in the system considered here), indicating that energy dissipation by local deformation processes contributes overwhelmingly the greater part of the measured energy of failure. This is, of course, the same reasoning as is used to explain why the bulk fracture energy of most solids is much greater than predicted by a pure Griffith criterion.

At low peel energies (of order 1–30 J m^{-2}) the failure path in a PET–Al–PET laminate remains on one side of the metallic layer, with the metal-carrying side itself covered with a thin layer of organic material stripped from the opposite surface, which XPS measurements indicate to be at least 10 mm thick.[5] At higher energies the failure path alternates from side to side of the metallic layer.[2] The relatively low peel energies associated with the former failure mode are still more than 2 orders of magnitude above the 0.1 J m^{-2} accounted for by surface energy considerations, so that considerable additional energy dissipation is taking place here—perhaps involving the deformation and removal of a "weak boundary layer," a concept developed by Bikerman[7] (though see, e.g., the reviews of Kinlock[8] and Wu[9] for a critical appraisal of the idea). Such a mechanism could be associated with the presence on the surface of oligomers, notably cyclic trimer, which are present in bulk PET in an equilibrium concentration of 1–1.5 wt% and which readily migrate to the surface,[10,11] or simply with highly orientated PET which is

easily detached from the main body of the film. Alternatively, surface contaminants offer a potential weak boundary layer. Gibbins and Windle[2] showed using X-ray photoelectron spectroscopy that in some samples the fracture path ran between the PET and a hydrocarbon contaminant layer, while in others it appeared to propagate within the PET although remaining close (perhaps 1 nm) to the aluminum layer. In higher strength laminates fabricated after suitable glow discharge pretreatment, peel testing leaves the aluminum distributed over both halves of the failed laminate.

In general, the measured peel energies are insensitive to the thickness of the deposited metal layer.[5]

Fractography of Peel Failure

The polymer–metal–polymer (PMP) geometry facilitates the peel testing of well-bonded specimens—up to the point where failure occurs by bulk tearing, corresponding to peel energies of around 800 J m^{-2} in 50 μm thick film. Figure 4 shows a typical failure surface for a specimen with peel energy 600 J m^{-2}. The peel path alternated from side to side of the aluminum layer as illustrated in Figure 5, and several distinctive features of the surface can be identified.

We first consider the circular areas, typically 200 μm in diameter, in Figure 4. These are associated with dust particles present on the film surface during lamination (some are still visible) and the absence of any evidence of plasticity indicates poor or nonexistent metal–metal bonding in these regions. Their extent, 1–2 orders of magnitude greater in area than the projected area of the dust particles themselves, underlines the dramatically detrimental effect which dust may have on bond performance, and hence the importance of its exclusion in commercial use.

Secondly, we note that the surface displays relief on a scale very much greater than the thickness of the deposited metal (some tens of nanometers), indicating extensive plastic deformation in a region of the polymer film several microns in depth. Even in a specimen with a relatively low peel energy (Fig. 6), some areas display relief of this type. Such results suggest that an important feature of the PMP laminate is that the evaporated aluminum can bond the two PET films so strongly that subsequent failure proceeds by a cohesive route within the PET, which may deviate well away from the aluminum layer. The difference between the specimens illustrated in Figures 4 and 6 is then essentially quantitative. Substantial "tongues" of material—up to perhaps 100 μm across—stand out above the level of the surrounding surface, and there is a tendency for a set of such features (for example, at *A* in Fig. 4) to be formed when the "crack" front has reached a certain point. One example, in the upper left of Figure 4, is enlarged in Figure 7. The reentrant cavity underneath the "tongue" indicates a change in fracture plane, perhaps associated with a region of weak boundary around a dust particle. The "tongue" represents the remains of the ligament formed from the material between the original main crack and the start of the new one. Figure 8 summarizes the process postulated.

A third feature of the failure surface in Figure 4 is the presence of fine striations more-or-less perpendicular to the peel direction. Closer examination

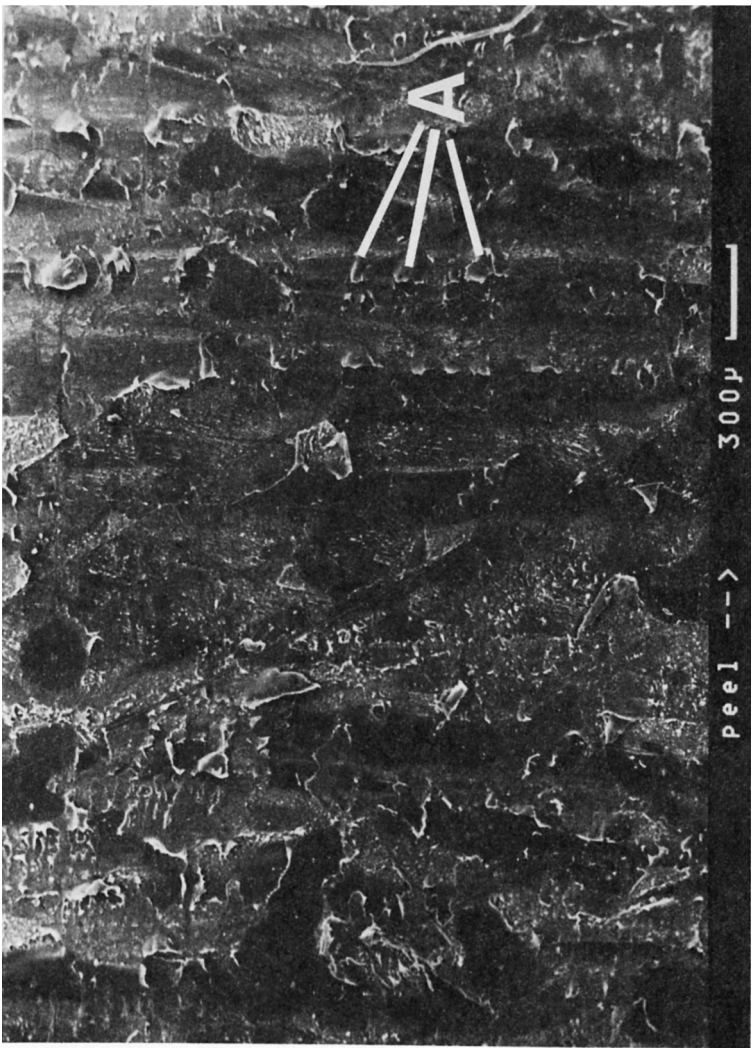

Fig. 4. SEM micrograph of a 600 J m^{-2} peel surface. The arrow indicates the direction of peel. Note the circular regions around dust particles where metal-metal bonding has not been achieved, and the partial detachment of "tongues" of material, often at particular crack-front positions (e.g., at *A*).

Fig. 5. Transmitted-light optical micrograph of a specimen similar to that of Fig. 4. Light areas carry no aluminum layer; circular dark areas (typically around dust particles) are those where metal-metal bonding was not achieved, and which therefore retain one layer thickness of deposited aluminum; irregular dark areas are those where failure occurred on the other side of the aluminum layer leaving a "double thickness" of metal.

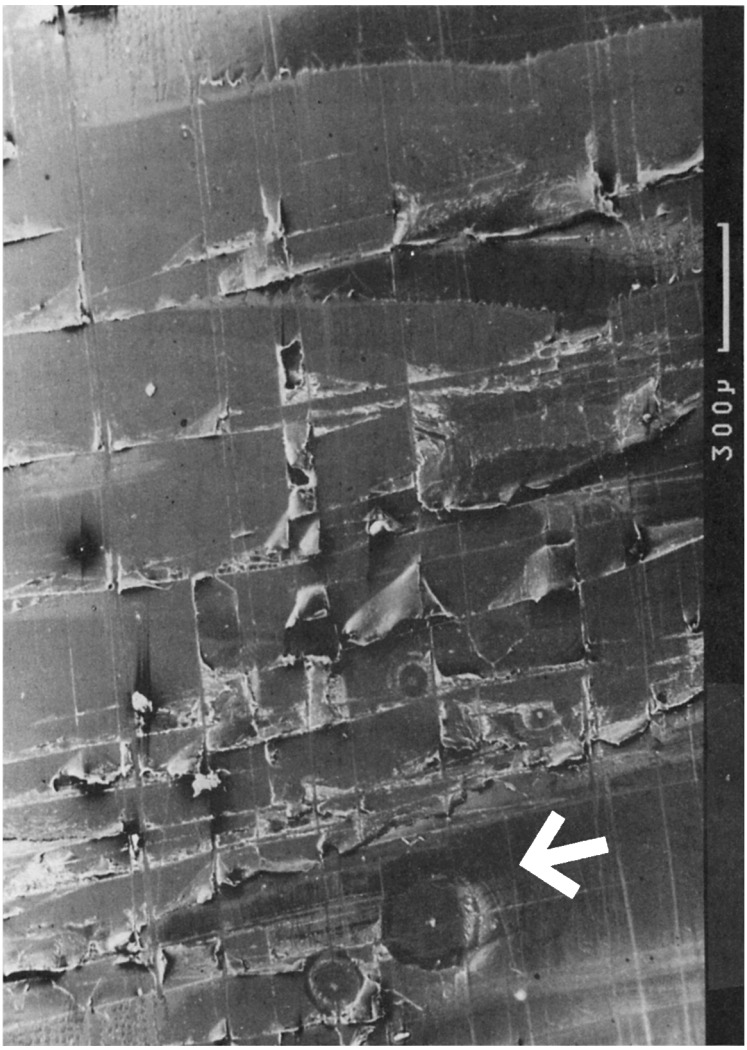

Fig. 6. SEM micrograph of a low energy (50 J m^{-2}) peel surface, indicating isolated areas of extensive plasticity. The arrow indicates the direction of peel.

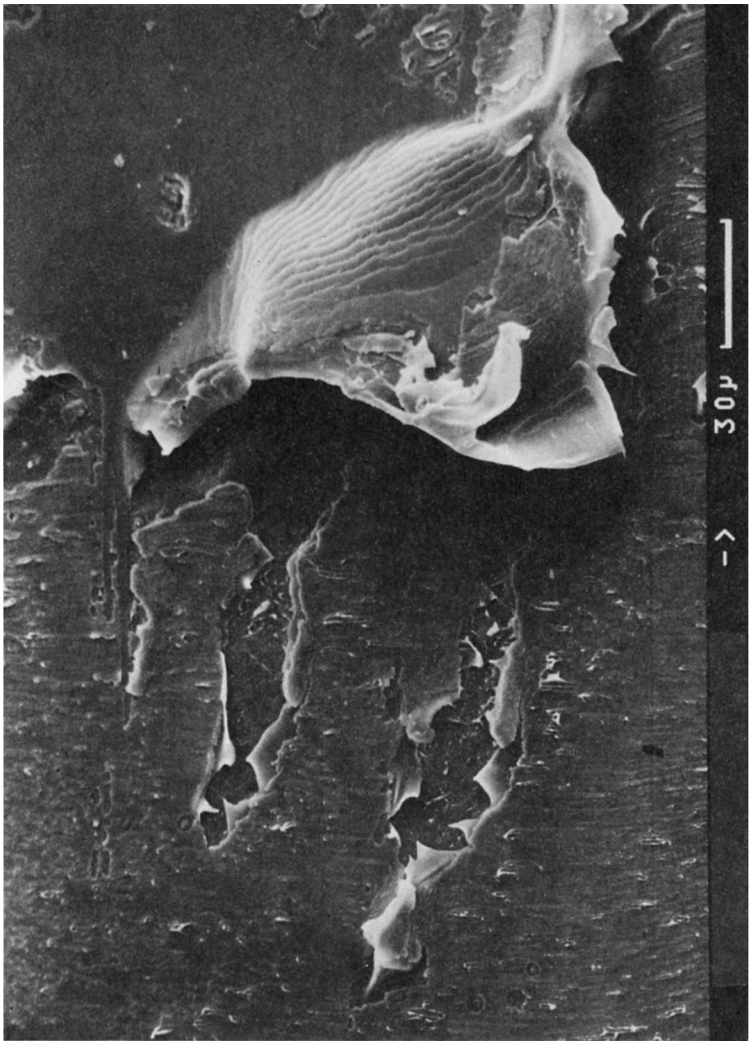

Fig. 7. Macroductility: detail of the feature denoted *C* in Figure 4. The arrow indicates the direction of peel. The probable position of a dust particle is indicated by the depression in the otherwise featureless area at top right.

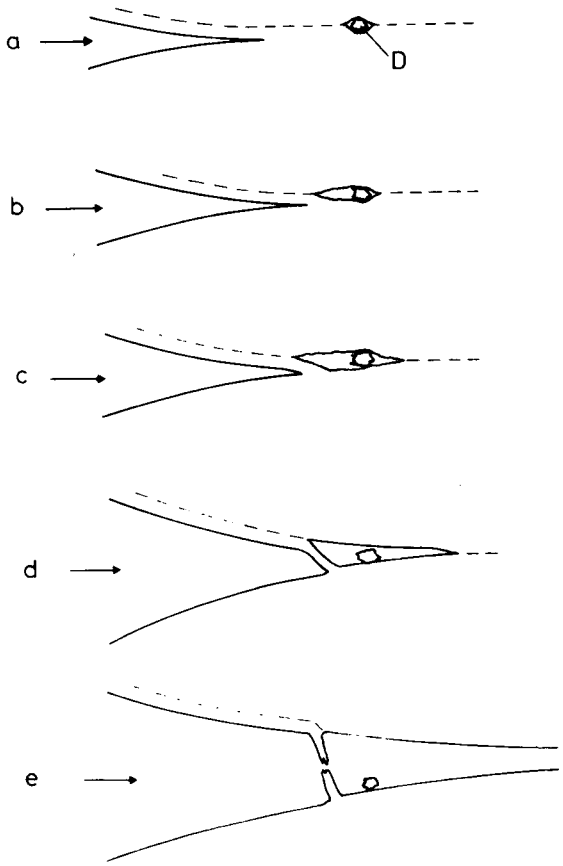

Fig. 8. Schematic representation of the fracture process leading to Figure 7. The arrow indicates the peel direction, and the dashed line the position of the aluminum layer: (i) peel "crack" approaches a poorly bonded region: in this example it is associated with dust particle *D*; (ii) void opens up around dust particle; (iii) void tip takes over as new crack front; (iv) with further peeling material between old and new cracks is drawn out to form a ligament; (v) eventual breakage of ligament.

(Fig. 9) reveals these to be due to ridges formed by ductile tearing on a scale of a few microns (in terms of ridge separation). The detailed appearance varies from area to area, with some regions displaying well-defined ridges while others exhibit irregular tearing. These variations suggest local changes in the crack path with respect to the PET crystallites, though local variations in crystallinity, the degree of crystallite orientation, and crystallite size may also play a part. In regions such as Figure 10, surface deformation is localized in narrow bands. These may be associated with the lamellar structure of the biaxially drawn PET film, the lamellae having intersected the fracture plane at a shallow angle. For brevity, we will use the term macroductility to describe the formation of features such as Figure 7, resulting from the linking up of the main peel front with local voids and often involving a change of fracture plane, and the term microductility to refer to the fine tearing, on a scale of order 1 μm, associated with propagation of a single crack front.

Fig. 9. Microductility: fine scale ductile tearing within the surface regions of the PET film. The arrow at lower left indicates the peel direction.

Figure 11 illustrates a combination of macroductile and microductile behavior, where large "islands" of PET have been torn out of the opposite half of the laminate (examination of the mating half of the laminate supports this view). On the surface of these "islands," microductile tearing is evident.

The relatively minor role of the metal layer in determining the failure morphology is underlined by Figures 12 and 13. These depict a laminate formed by an amended procedure, including operation of the tungsten filaments but without loading a fresh charge of aluminum. Inevitably traces of aluminum would be present and probably assisted the bonding, but the optical density was not more than 0.2, indicating a thickness of metal less than 2 nm. Nevertheless, a mean energy of 100 J m^{-2}, and a peak value of 300 J m^{-2}, were recorded, and the fractographic features of the peel failure surface are essentially the same as those described previously.

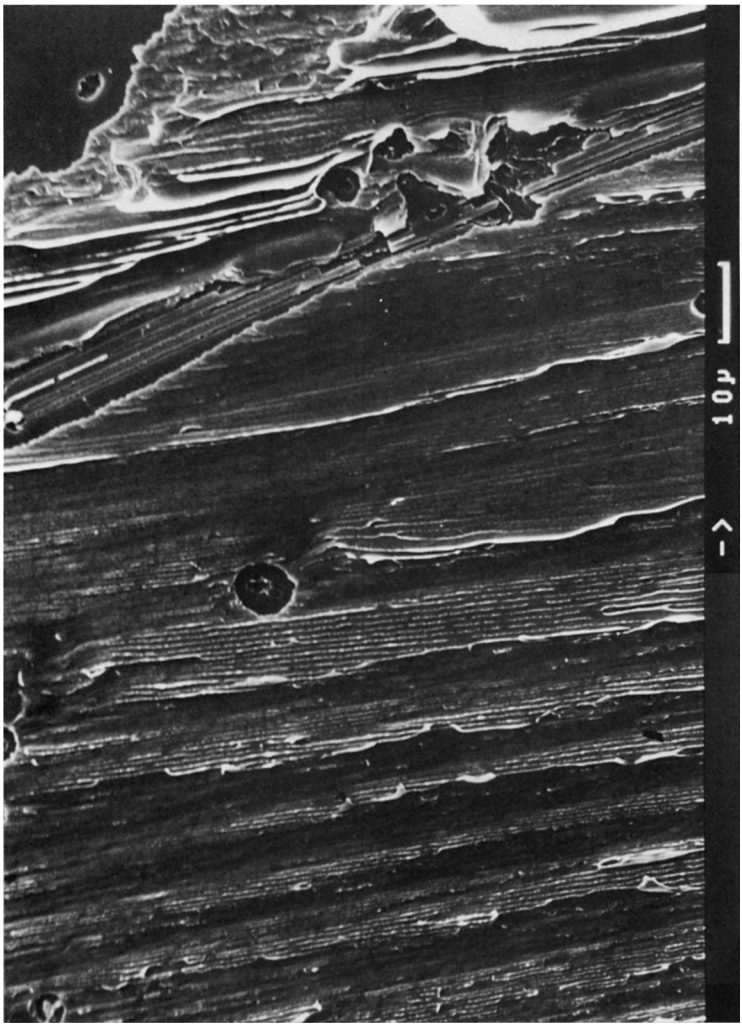

Fig. 10. Striated fracture surface which may be associated with the lamellar structure of the PET film. The arrow indicates the peel direction.

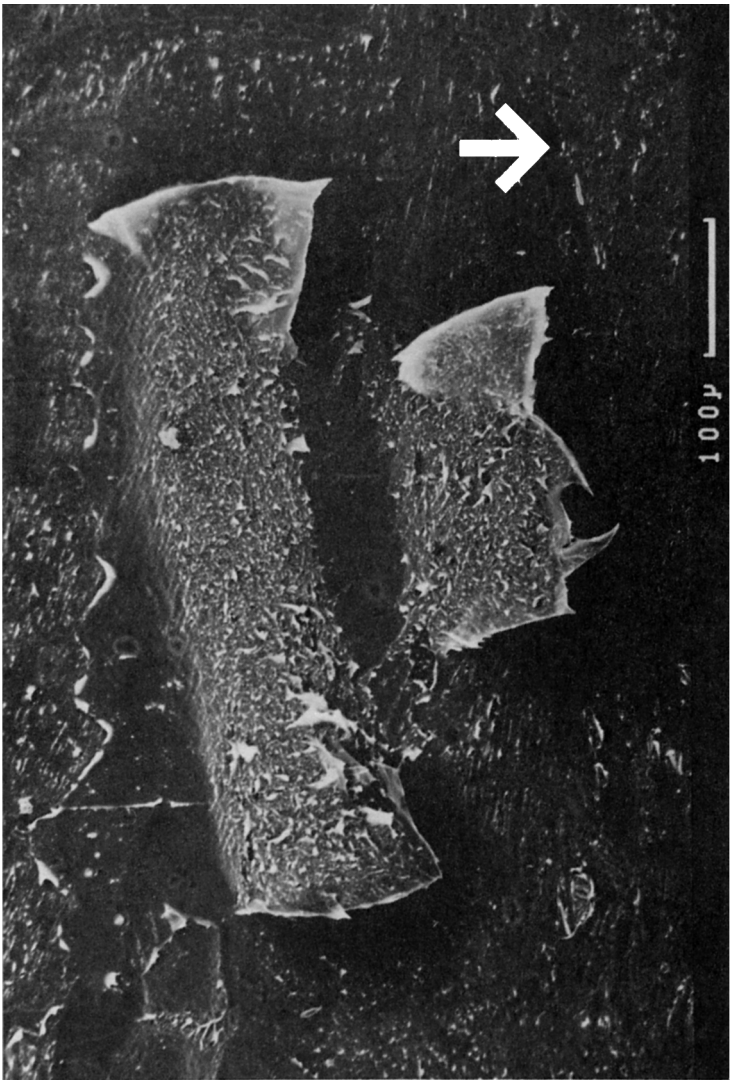

Fig. 11. Combination of macroductile and microductile behavior: failure energy approximately 500 J m^{-2}. The arrow indicates the peel direction.

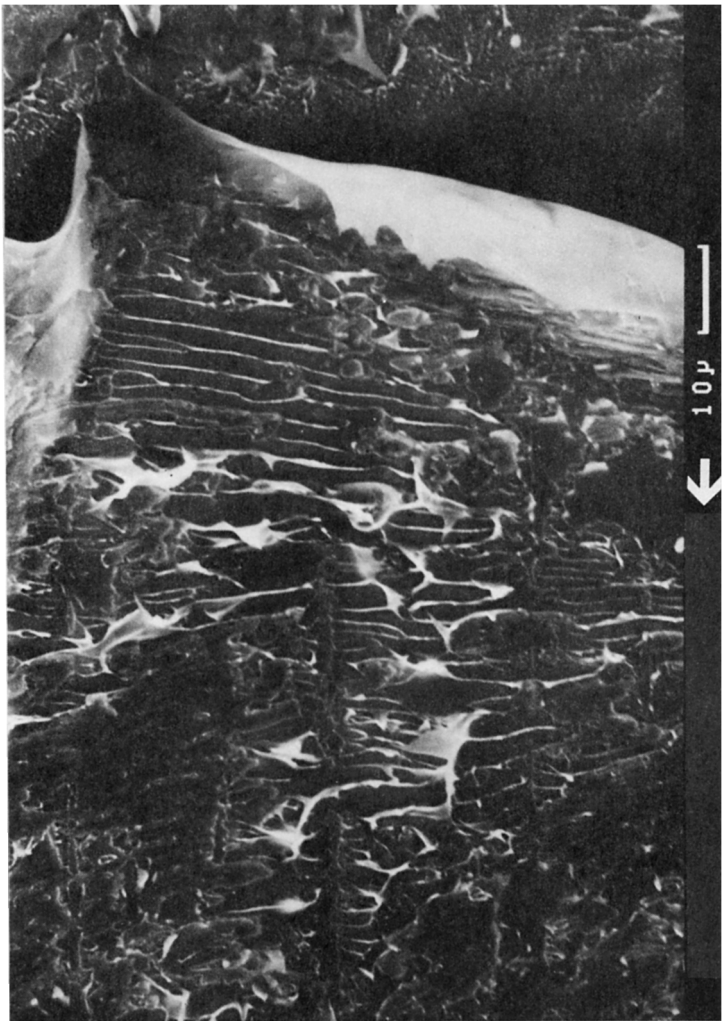

Fig. 12. Macroductile and microductile behavior in an "autohesive" PET laminate. The arrow indicates the peel direction.

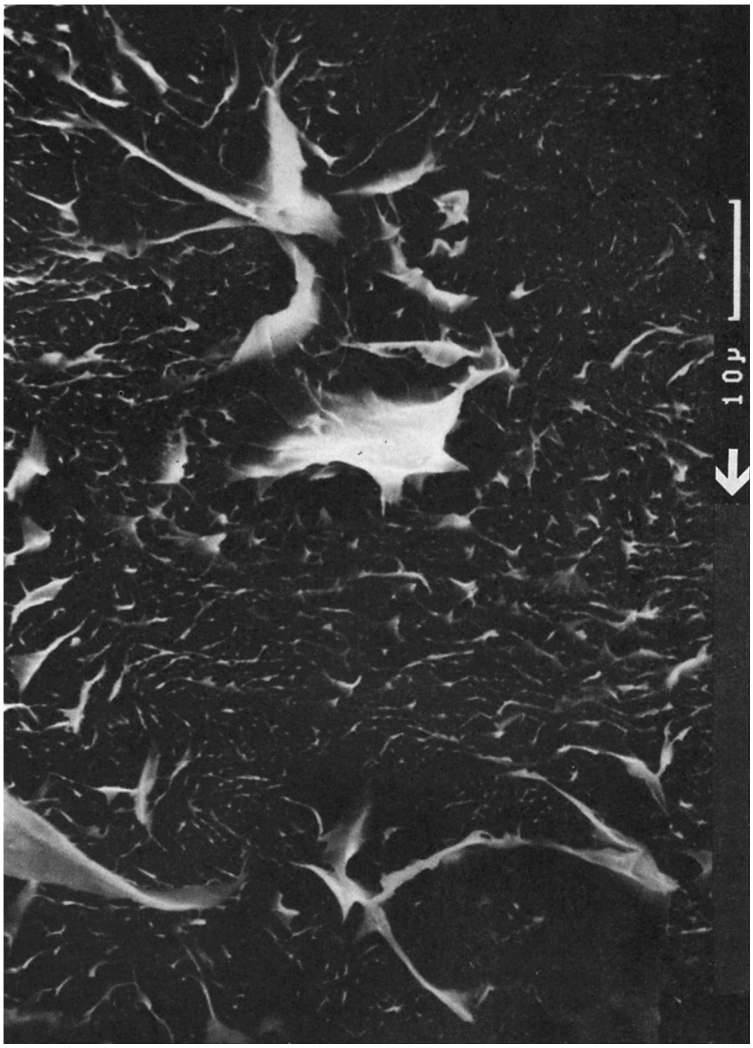

Fig. 13. Close-up of ductile tearing on the laminate illustrated in Figure 14.

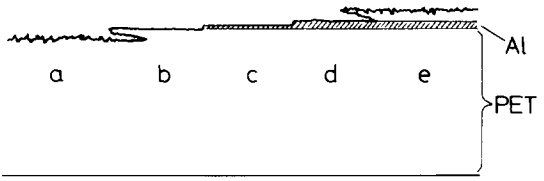

Fig. 14. Possible regions of the failure surface: (a) surface layer removal from the lower PET film; (b) failure at (or close to) the lower PET–Al interface; (c) less successful lamination—original Al coating retained; (d) failure at (or close to) the upper PET–Al interface; (e) surface layer removal from the upper PET film. The aluminum thickness is greatly exaggerated.

Mechanisms of Peel Crack Propagation

The scale of the macroductile surface relief indicates that the failure path may deviate from the interface by distances which are large compared to the metal thickness, so that the failure surface will comprise regions of several types, illustrated schematically in Figure 14:

(i) areas where surface layers have been removed, exposing "bulk" PET;
(ii) areas where the surface layers of PET have remained intact or have been only partially removed, with failure between PE and aluminum exposing the original surface of the PET;
(iii) areas where successful bonding has not been achieved (e.g., owing to dust inclusion): both surfaces will retain their aluminum coating.

With the proviso that an apparent aluminum surface may carry an organic "weak boundary layer" stripped from the PET, a combination of such regions would account for the irregular surface appearance observed by Gibbins and Windle[2] and associated with discontinuous propagation of peel failure.

Changes in fracture plane, and the consequent deformation and breakage of ligaments as illustrated in Figure 8, provide an important mechanism of energy dissipation. The frequency of these changes, and the possibility of significant deviations of the crack path from the metal layer, indicate that the necessary debonding ahead of the peel front can occur not only in the presence of foreign particles, but on a more widespread scale involving the formation of microcracks on a variety of planes in the vicinity of the advancing peel crack tip. Such a mechanism has been confirmed by peel experiments performed inside the chamber of a SEM, to be reported separately.[12] Analogies may be drawn with the "advance microcracking" reported by Bascom et al.[13] in aluminum—epoxy bonds, and with lamellar tearing in rolled steels. There is also the interesting implication that films with a lamellar microstructure may have enhanced adhesive properties on account of the many competing fracture paths close to and parallel to the bonded surface.

This microcracking would presumably take place in the tensile stress field ahead of the crack tip: a qualitative idea of the stress distribution can be gained from Figure 15, drawn from work on the average stresses (normal to the fracture plane) in a Hookean adhesive layer bonding two metal strips and subjected to a peel test.[14–17]

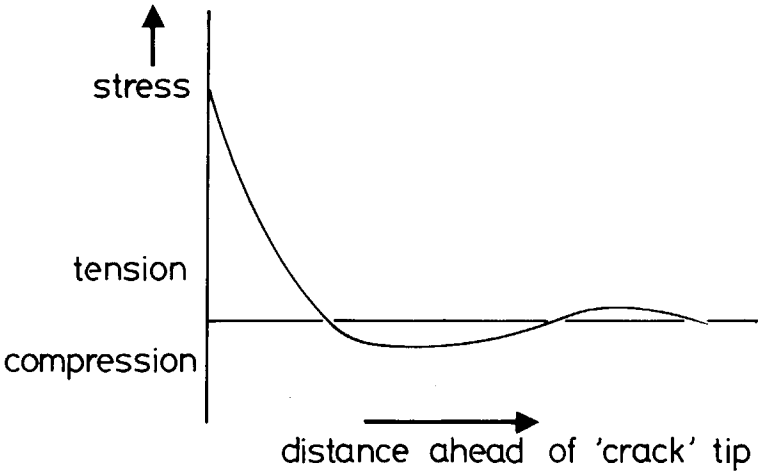

Fig. 15. Schematic illustration of the stress normal to the interface ahead of a peel crack tip. The stress alternates between tension and compression.

On a finer scale, microductile tearing will involve failure between oriented groups of crystallites, and this will be true whether we are dealing with the growth of the main crack or with localised voiding. High failure strengths would be promoted by making this requirement as energy-costly as possible, perhaps by reducing the levels of crystallite perfection and orientation in the surface regions of the film in order both to increase the energy per unit area for failure along a given plane, and to encourage the formation of many small microcracks rather than the extensive propagation of a single one. Additionally, the overall failure energy would be raised by increasing the typical depths into the film at which local failure occurs, and hence the average depth down to which extensive plastic deformation takes place.

CONCLUSIONS

1. The polymer–metal–polymer laminate geometry has proved successful in making clear the main features of peel failure near a PET–aluminum interface, right up to the stage at which bulk tearing of the base film occurs first, and in providing data on the energies associated with peel failure.

2. At high laminate strengths (several hundred joules per square meter), fracture is principally cohesive, often proceeding at a depth of several microns into the PET film, and is accompanied by extensive plastic deformation.

3. Fractographic studies indicate that the propagating peel "crack" is able to transfer from one plane to another, the aluminum–PET interface being only one of the possible routes.

4. This transfer may be interpreted in terms of microcracking in the vicinity of, but not contiguous with, the main peel crack. Further peel propagation will then require the deformation of relatively large volumes of PE (macroductility).

5. Further enhancement of peel strengths associated with metal–polymer bonding may require study and possible modification of local molecular and crystallite orientation within the PET film.

The work described was supported by ICI PLC, Petrochemicals and Plastics Division, who also supplied the "Melinex" film.

References

1. N. J. Gibbins and A. H. Windle, *Mater. Sci. Technol.*, **1**, 263 (1985).
2. N. J. Gibbins and A. H. Windle, *J. Mater. Sci.*, to appear.
3. U. K. Pat. No. 8030724.
4. E. H. H. Jamieson and A. H. Windle, *J. Mater. Sci.*, **18**, 64 (1983).
5. N. J. Gibbins, Ph.D. dissertation, University of Cambridge, 1981.
6. D. G. Rance, in *Surface Analysis and Pretreatment of Plastics and Metals*, D. M. Brewis, Ed., Applied Science, London, 1982, p. 139.
7. J. J. Bikerman, *The Science of Adhesive Joints*, Academic, New York, 1961 and 1968.
8. A. J. Kinlock, *J. Mater. Sci.*, **15**, 2141 (1980).
9. S. Wu, *Polymer Interface and Adhesion*, Dekker, New York, 1982, Chap. 12, p. 449.
10. S. D. Ross, E. R. Coburn, W. A. Leach, and W. B. Robinson, *J. Polym. Sci.*, **13**, 406 (1954).
11. I. Goodman and B. F. Nesbitt, *Polymer*, **1**, 384 (1960).
12. D. J. Brown, A. H. Windle, D. G. Gilbert, and P. W. R. Beaumont, *J. Mater. Sci.*, **21**, 314, (1986).
13. W. D. Bascom, C. O. Timmons, and R. L. Jones, *J. Mater. Sci.*, **10**, 1037 (1975).
14. G. J. Spies, *Aircraft Eng.*, **28**, 64 (1953).
15. D. H. Kaelble, *Trans. Soc. Rheol.*, **3**, 161 (1959).
16. D. H. Kaelble, *Trans. Soc. Rheol.*, **4**, 45 (1960).
17. D. H. Kaelble, *Trans. Soc. Rheol.*, **9**, 135 (1965).

Received April 22, 1986
Accepted January 5, 1987